FOREWORD

This report was prepared by The University of New Mexico for Contract AF 29(601)-5976. Principal investigator for this contract is Dr. W. W. Grannemann. Other investigators are Dr. Harold D. Southward, Dr. William J. Byatt, Dr. Llewellyn Boatwright, Harold Cates, Goebel Davis, Arthur Golubiewski, and LeRoy Meyer.

The authors wish to acknowledge the assistance of A1c A. H. Hoffland and A1c P. L. Kowieski in operating the flash X-ray system.

ABSTRACT

A review of the basic theory of Hall effect and Hall effect devices as related to transient radiation effects is presented. The theory predicts that any transient effect in the Hall voltage output during gamma irradiation of the device depends on the type of biasing used. There is no change in Hall voltage output for constant voltage bias, but the Hall voltage varies as a function of $1/n$ for constant current bias, and as a function of $|1/\sqrt{n}|$ for constant power bias where n is the number of free electrons/cm^3 in the material. The transient radiation effects are small and usually within the noise level for dose rates up to 10^7 r/sec. Some experimental data have been obtained using the AFWL 600-kv flash X ray and WSMR 8-Mev Linac that support the theory. Both thin film and crystal devices were used. The thin film devices appear to have a wider range of frequency response and are more radiation resistant.

PUBLICATION REVIEW

This report has been reviewed and is approved.

Karl H. Schumaker

KARL H. SCHUMAKER
Captain USAF
Project Officer

John W Talley

JOHN W. TALLEY
Lt Colonel USAF
Chief, Nuclear Power Branch

R. A. HOUSE
Colonel USAF
Chief, Development Division

CONTENTS

ILLUSTRATIONS

TABLES

1. INTRODUCTION

In 1878, Hall found that the stream lines of an electric current in a metallic conductor were distorted when the conductor was placed in an external magnetic field. This distortion arises from an electric field set up at right angles to the current and to the magnetic field. The effect is well known in conductors and semiconductors, for both steady state and low frequencies. Figure 1 illustrates the polarities of the Hall voltage for I_x in the direction of conventional current flow.

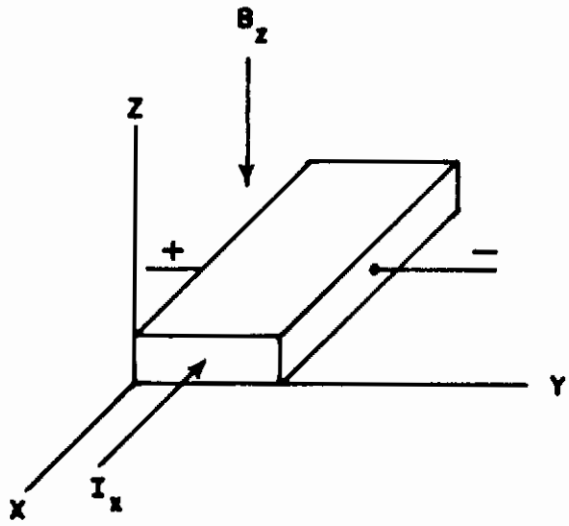

Figure 1. Hall voltage direction

Since the late 1950's, commercial Hall devices have been available and have found important application in the field of instrumentation. The Hall effect itself is important from the standpoint of revealing the mechanisms of conduction in semiconductors. This makes it a valuable tool in radiation studies. When data from the measurement of both Hall effect and conductivity are combined, the concentration and mobility of carriers can be determined if the material is cooled to liquid nitrogen temperature. A Hall effect arising from displacement current in dielectrics should also exist,

and if it could be detected might offer a new approach in radiation effect studies of dielectrics.

Some of the applications of Hall devices include the following: flux meters, compasses, magnetometers, clip-on DC ammeters, galvanometer amplifiers, Hall effect multipliers, computer elements, modulators, AC power meters, electric torque measurements, Hall effect amplifiers, Hall effect displacement devices, Hall gyrators, wave analyzers, isolators, magnetic tapereaders, microwave power measurement, resolvers, varmeters, variable attenuators, frequency multiplexing, and DC to AC conversion.

The purpose of this study is to more fully understand the transient radiation effects on Hall devices, with the ultimate goal of improving instrumentation in nuclear environments.

The commercial Hall devices used in this study are the Ohio Semiconductors Halltrons, and the Beckman thin-film Hallefex voltage generators. These are indium antimonide and indium arsenide devices. The Halltron HS-51 and Hallefex 350 are the InSb devices, and the Halltron HR-31 and Hallefex 351 are the InAs devices used. Also, some InSb Hall devices were made in the University of New Mexico Laboratory with special noninductive leads.

2. THEORY OF HALL DEVICES

a. Hall effect for metals and impure semiconductors

The most straightforward derivation of the Hall coefficient is obtained by assuming the charge carriers are all one type and are particles. The Hall coefficient (defined by equation (7) below) can be obtained for the Lorentz force equation as follows:

$$\vec{F}_y = e(\vec{E}_y - \vec{v}_x \times \vec{B}_z) = 0 \tag{1}$$

$$eE_y = ev_xB_z \tag{2}$$

$$E_y = v_xB_z \tag{3}$$

where

F_y = force in y direction,

e = charge of electron,

E_y = electric field intensity in the y direction,

v_x = drift velocity of carrier in x direction, and

B_z = magnetic field in z direction.

The equation for current density, J_x, can be written as

$$J_x = en\,v_x \tag{4}$$

$$v_x = \frac{J_x}{en} \tag{5}$$

where n = the number of electrons.

Combining equations (5) and (3) we have

$$E_y = \frac{J_x B_z}{en} = R_h J_x B_z \tag{6}$$

where R_h is the Hall coefficient defined as the ratio of E_y to $J_x B_z$. Then

$$R_h = \frac{E_y}{J_x B_z} = \frac{1}{en} \qquad m^3/\text{coul} \; . \tag{7}$$

The number of electrons can be computed from equation (7); thus

$$n = \frac{B_z J_x}{eE_y} \tag{8}$$

The relationships of mobility (μ), resistivity (ρ), and the Hall coefficient (R_h) can now be obtained. First we will develop the equations for μ and σ, the conductivity.

$$a = \frac{F}{m} = \frac{eE}{m} = \frac{v}{\tau} \tag{9}$$

$$v = e\tau E/m \tag{9a}$$

where a = acceleration, F = force, m = mass, e = charge of an electron, E = field intensity, v = velocity, and τ = average time between collisions. Then using equation (4) we can get the expression for conductivity:

$$J = env = \frac{e^2 n\tau}{m} E = \sigma E \tag{10}$$

from which

$$\sigma = \frac{e^2 n\tau}{m} \tag{11}$$

The equation for mobility can similarly be obtained from

$$\mu = \frac{v_{ave}}{E} = \frac{\tau e}{m} \tag{12}$$

Next taking the ratio of μ to σ, we obtain R_h

$$\frac{\mu}{\sigma} = \frac{1}{ne} = R_h \tag{13}$$

or

$$R_h = \frac{1}{ne} = \frac{\mu}{\sigma} = \mu\rho \tag{14}$$

The Hall voltage equation may be obtained from equation (6) and is given by

$$V_h = \frac{R_h BI}{d} \tag{15}$$

where

V_h = Hall voltage (volts),

R_h = Hall coefficient $\left(\frac{m^3}{coul}\right)$,

B = magnetic field $\left(\frac{Weber}{m^2}\right)$,

I = current (amperes), and

d = thickness of the material (meters).

b. Corrections on the Hall formulas for semiconductors

For most semiconductors, equation (7) has to be corrected because τ is not the same for all electrons due to lattice scattering and electrons not being entirely free electrons. The correction comes from the statistics involved, and is given by $\frac{3\pi}{8}$. The Hall coefficient for n-type material is

$$R_h = -\frac{3\pi}{8}\frac{1}{ne} \tag{16}$$

For strongly p-type material we have

$$R_h = +\frac{3\pi}{8}\frac{1}{pe} \tag{17}$$

where p is the hole concentration.

A similar expression can be obtained for Hall mobility,

$$\mu_h = \frac{3\pi}{8}\mu \tag{18}$$

c. Hall angle (θ)

The Hall angle is determined by the circular path the electron traverses before it is scattered by a collision with an atom. The time corresponding to this path is the collision time τ'. The Hall angle is

related to τ' by

$$\theta = \omega\tau' = \frac{eB_z\tau'}{m} = \mu_h B_z \tag{19}$$

For small angles, θ can be related to the x and y components of E by

$$\frac{E_y}{E_x} = \frac{B_z e\tau'}{m} = \theta \tag{20}$$

The size of θ is a property of the material and μ_h. The Hall mobility is often defined as the Hall angle per unit magnetic field. In equation form it is

$$\mu_h = \frac{\theta}{B} = \frac{e\tau'}{m} \tag{21}$$

d. Hall coefficient when both electrons and holes are present

If the total current is made up of electrons and holes, then the total current density is given by the expression

$$J_T = J_n + J_p \tag{22}$$

The component of current density in the y direction is

$$J_y = J_{ny} + J_{py} = B_z eE_x\left(-n\mu_n^2 + p\mu_p^2\right) \tag{23}$$

From equations (7) and (23) the Hall coefficient can be shown to be

$$R_h = \frac{3\pi}{8e}\,\frac{\left(-n\mu_n^2 + p\mu_\rho^2\right)}{\left(\mu_n n + \mu_\rho p\right)^2} \tag{24}$$

Let $b = \frac{\mu_n}{\mu_\rho}$; then equation (24) is often seen as

$$R_h = \frac{3\pi}{8} e \frac{-nb^2 + p}{(nb + p)^2} \tag{25}$$

e. Relation between Hall voltage (V_h), number of carriers (n) and mobility (μ)

From the Hall voltage equation and the equation for power we have

$$V_h = \frac{R_h BI}{d}$$

$$P = I^2R$$

$$P = I^2R = I^2 \frac{\rho \ell}{A} = I^2 \frac{\rho \ell}{wd}$$

where the dimensions are shown in figure 2.

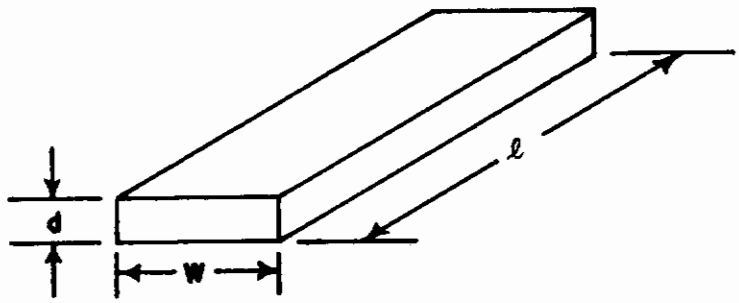

Figure 2. Hall device dimensions

Then using the relation $R_h = \mu\rho$, we get

$$\frac{V_h}{B} = \mu\sqrt{\frac{Pw\rho}{\ell d}} = \mu \rho^{1/2} \left(\frac{Pw}{\ell d}\right)^{1/2} \tag{27}$$

$$= \frac{\mu}{(e\mu n)^{1/2}} \left(\frac{Pw}{\ell d}\right)^{1/2} = \left(\frac{\mu}{n}\right)^{1/2} \left(\frac{Pw}{e\ell d}\right)^{1/2} \tag{28}$$

Equation (27) indicates that to get a high V_h we would want to use a material with large μ and ρ. Equation (28) gives the relation between μ, n and V_h.

f. Temperature effect on the Hall coefficient

The Hall coefficient can be written as the ratio of mobility to conductivity and therefore will vary as $\mu(t)$ and $\sigma(t)$. The equation is

$$R_h = \frac{\mu_h}{\sigma} = \frac{3\pi}{8} \frac{'\mu}{\sigma} \quad . \tag{29}$$

A curve of Hall coefficient versus temperature for the Ohio Semiconductor InSb Hall probes is given in figure 3.

g. Magnetic field effect on the Hall coefficient

Experimentally it has been observed that there is no change in the Hall coefficient with magnetic field for n-type material.

3. PREPARATION AND CONSTRUCTION OF HALL PROBES

a. Semiconductor materials used in Hall devices

There are numerous semiconductor materials suitable for use in Hall devices. However, the III-V compounds offer the most desirable parameters of high mobility combined with high resistivity and consequently a large Hall coefficient. In equation (27) it was shown that the Hall voltage is given by

$$V_h = B \mu \rho^{1/2} K$$

where V_h = Hall voltage, B = magnetic field, μ = mobility, ρ = resistivity, and K is a constant for any given temperature. Of the III-V compounds, InSb and InAs have the highest Hall sensitivity. Take InSb, for example, and compare its properties with those of the group IV elements with the three valence bonds of indium and the five of antimony to give four bonds. Electrical and optical properties are similar to silicon and germanium. However, the

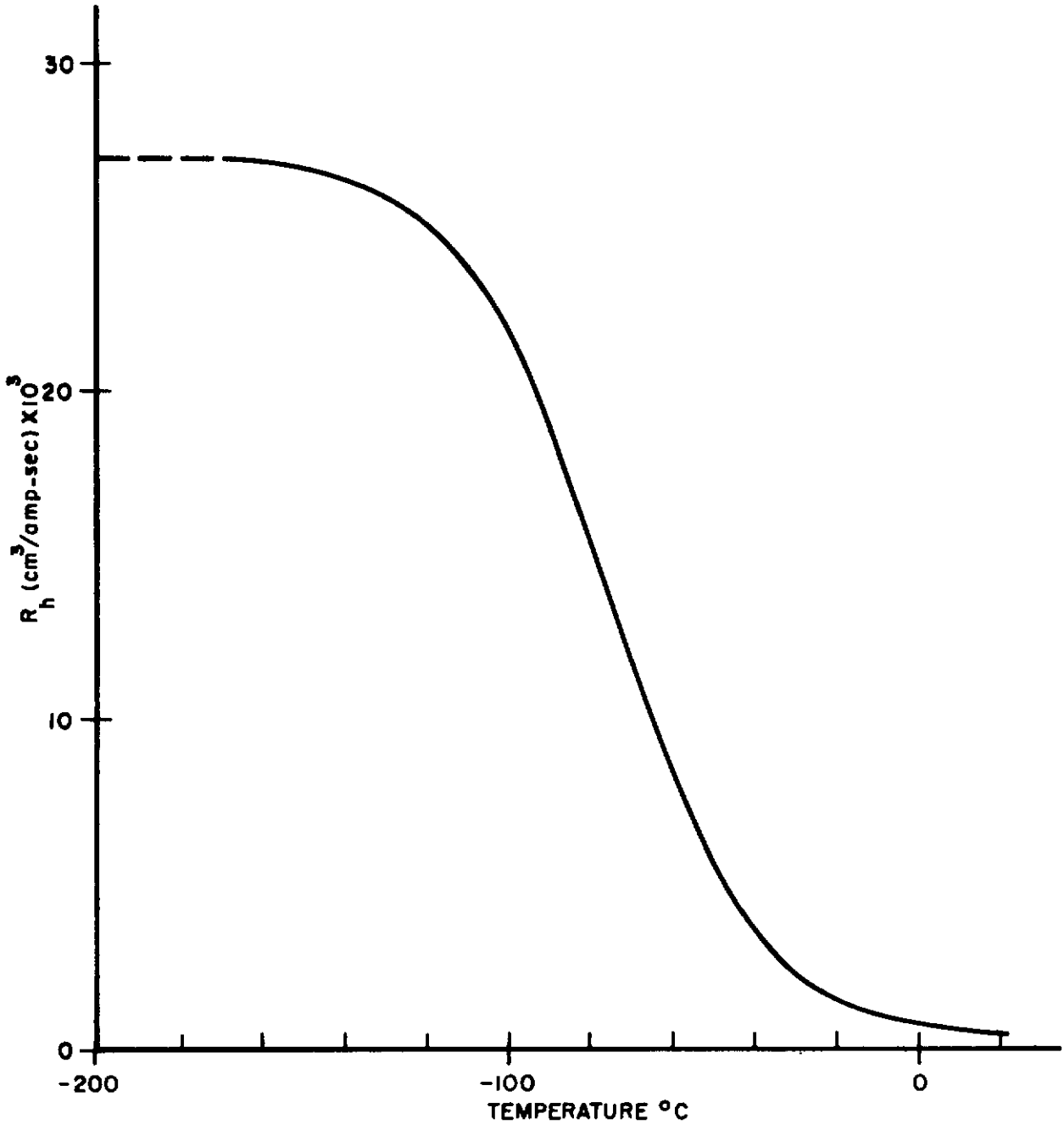

Figure 3. Curve of Hall coefficient vs. temperature for Ohio Semiconductor InSb Hall probe

magnitudes of important parameters underlying the physical properties of the bulk material are different.

In InSb it is not possible to obtain nonequilibrium carrier concentrations in bulk material at room temperature by injection, such as is done in junction devices, because it is necessary that a potential barrier exist. Therefore, it is not possible to make diodes and transistors using InSb at room temperature and above. The room-temperature lifetime of excess carriers in InSb is not governed by traps and recombination centers. Recombination occurs by the Auger effect or radiative processes. The recombination time is about 50×10^{-9} sec at 300°K. For most III-V compounds the radiative recombination rate is high, while for Ge and Si it is low. This is due to the different band structure.

The material properties of InSb, InAs, Ge, and Si are presented in table 1.

b. Construction details

The commercial bulk-type Hall devices usually have their lead arrangement such that there is an inductive loop. That is, if the magnitude of a pulsed magnetic field were to be measured, there would be an error due to the inductive pickup in the leads. Several Hall devices were made using special holders to reduce inductive pickup. The lead arrangement is shown in figure 4.

The probes were made in the form of rectangular plates of polycrystalline indium antimonide of grade InSb-8n which was obtained from Ohio Semiconductor Inc., Columbus, Ohio. This material has typical carrier concentration (n) of 4×10^{16} and mobility (μ) of 65,000 cm^2/volt-sec at room temperature, and maximum n of 5×10^{14} and minimum μ of 300,000 at 80°K. The rectangular plates were lapped down to a thickness of about 0.005 inch and then cut to the desired size of approximately 0.25 x 0.5 x 0.005 inch using an industrial "airbrasive" sand-blast unit.

Special attention was paid to contacts in preparation of the probes. It was necessary to produce an ohmic contact of the electrode metal with

Table 1

MATERIAL PROPERTIES

Property	InSb(n)	InAs(n)	Ge(n)	Si
n, carrier concentration at 300°K	4×10^{16}	5×10^{16}	2×10^{15}	10^{15}
at 80°K	1×10^{16}			
μ_n, electron mobility (cm^2/volt-sec) at 300°K	65,000	23,000	3,500	1,200
at 80°K	100,000			
μ_p, hole mobility at 300°K (cm^2/volt-sec)	1,000		2,000	
Atomic weight	118.39	94.87	72.6	28.09
τ, lifetime of excess carriers at 300°K (μsec)	50×10^{-3}		10-1,000	
ρ, resistivity (ohm-cm)	0.005	0.005	1	5
Temperature dependence of Hall coefficient (%/°C)	-2	-0.06	-0.01	-0.1
$R_h/\sqrt{\rho}$, figure of merit	6×10^3	2×10^3	3×10^3	3×10^3
Lattice constant (Å)	6.45			
Band gap (ev)	0.18			
m_e^*, effective mass of electrons	0.015	0.03		
m_n^*, effective mass of holes	0.18	0.30		
Specific heat over 0-100°C range (cal/gram/°C)	0.0533	0.0663	0.074	0.21
Melting point (°C)	523	942	958	1,430
Unit cell edge (Å)	6.48			
Interaction separation (Å)	2.80			
Density (gm/cm^3)	6.96	6.52	5.36	2.83

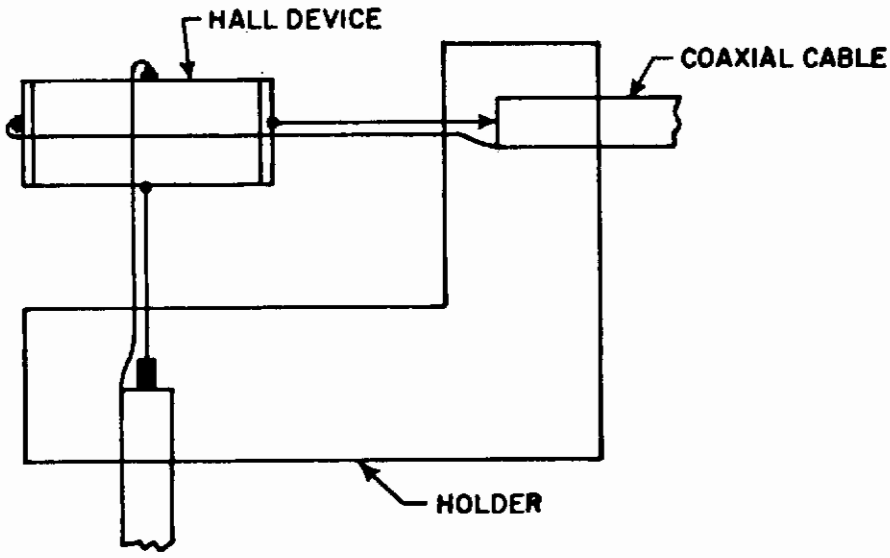

Figure 4. Noninductive Hall device holder

the indium antimonide. For this purpose the surface of the semiconductor was polished with emery powder, washed, and etched. The etching solution used was 2 pts. 70% HNO_3, 1 pt. 50% HF, 1 pt. 89% glacial Acetic Acid, and 2 pts. H_2O. The electrodes were then made using indium solder.

c. Frequency response

The frequency response of the Hall probes due to magnetic field changes has not been obtained due to lack of a good pulsed magnetic field source. However, the frequency response of the Hall device as a function of AC bias current has been obtained. The information from these response curves indicates that any changes in the characteristics of the Hall devices which are generated in the frequency range beyond the cutoff frequency will not be seen. This cutoff frequency can be related to the radiation pulse width by

$$f_c = \frac{1}{2T} \tag{30}$$

where

T = pulse width

f_c = cutoff frequency

A typical frequency response for bulk-type and thin-film devices is shown in figures 5 and 6, respectively. It appears that, in general, the thin-film devices have a broader bandwidth than the bulk-type devices. The bulk-type devices have a flat frequency response up to about 150 kc, and the thin-film devices to about 4 Mc. Beyond these cutoff points the device is usable only after careful balance networks are added, and then only for a very narrow bandwidth.

d. Compensating for frequency response

Figure 7 is a typical curve of the impedance change of a bulk-type Hall device as a function of frequency.

A displacement voltage appears at the Hall voltage terminals due to misalignment of leads and to thermal effects. The circuit of figure 8 may be used to compensate for this displacement voltage at low frequencies. At higher frequencies the compensating voltage will not cancel out the displacement voltage completely. This is due chiefly to the impedance and phase change of the Hall device. Additional compensation would be required because the magnitude and phase of the compensating voltage would have to be adjusted for each frequency for it to cancel out properly. If the bias current is DC, the displacement voltage will appear as a DC component and will be blocked by an AC amplifier when measuring a time-varying magnetic field.

e. Sensitivity

The sensitivity of a Hall device is usually given in terms of volts/ampere-kilogauss. Typical values are:

Haltron HS-51	0.1V/k gauss-amp
Hallefex 335	2V/k gauss-amp

The Hall voltage sensitivity can be increased by the use of flux

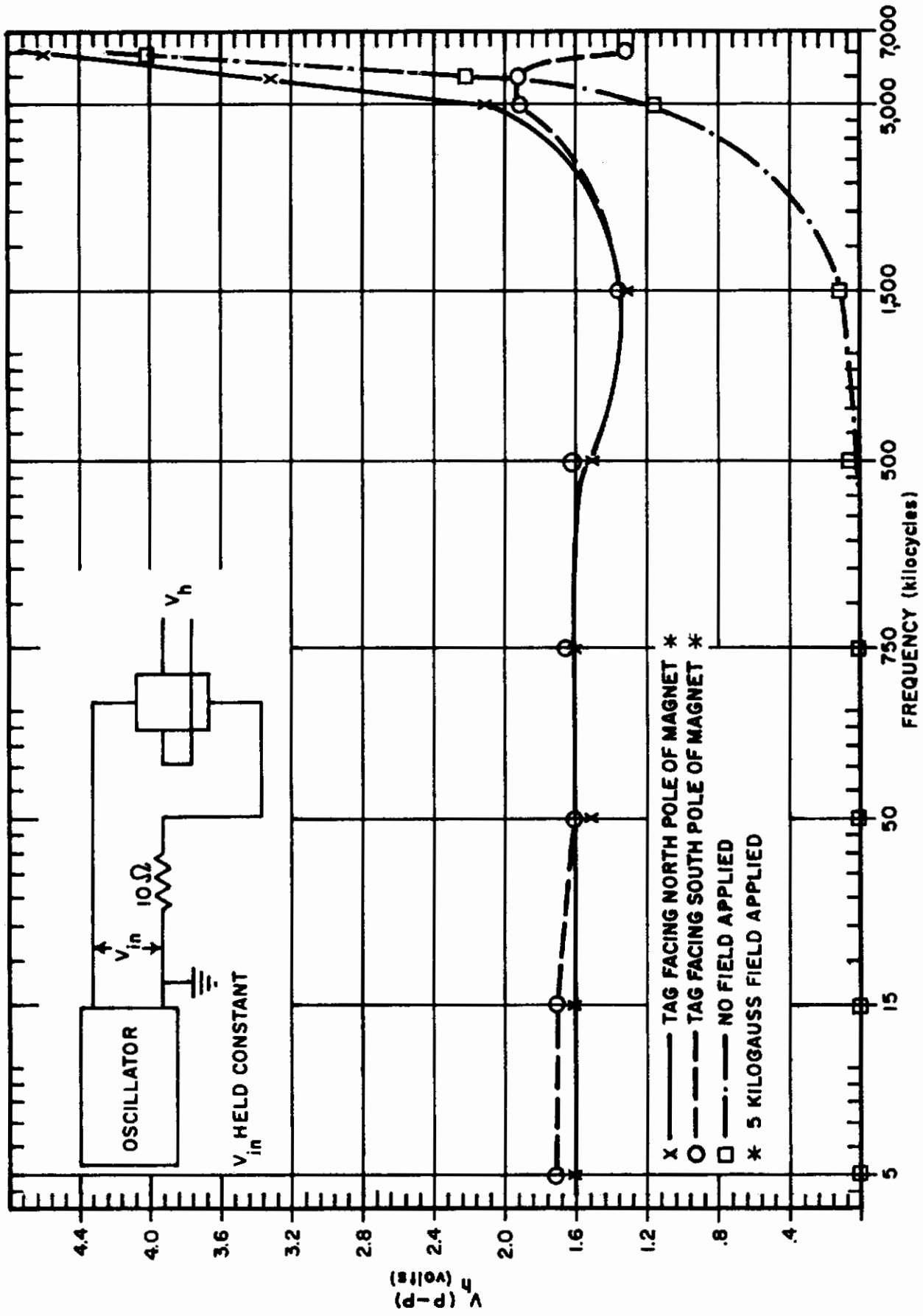

Figure 5. Frequency response of bulk-type Hall device

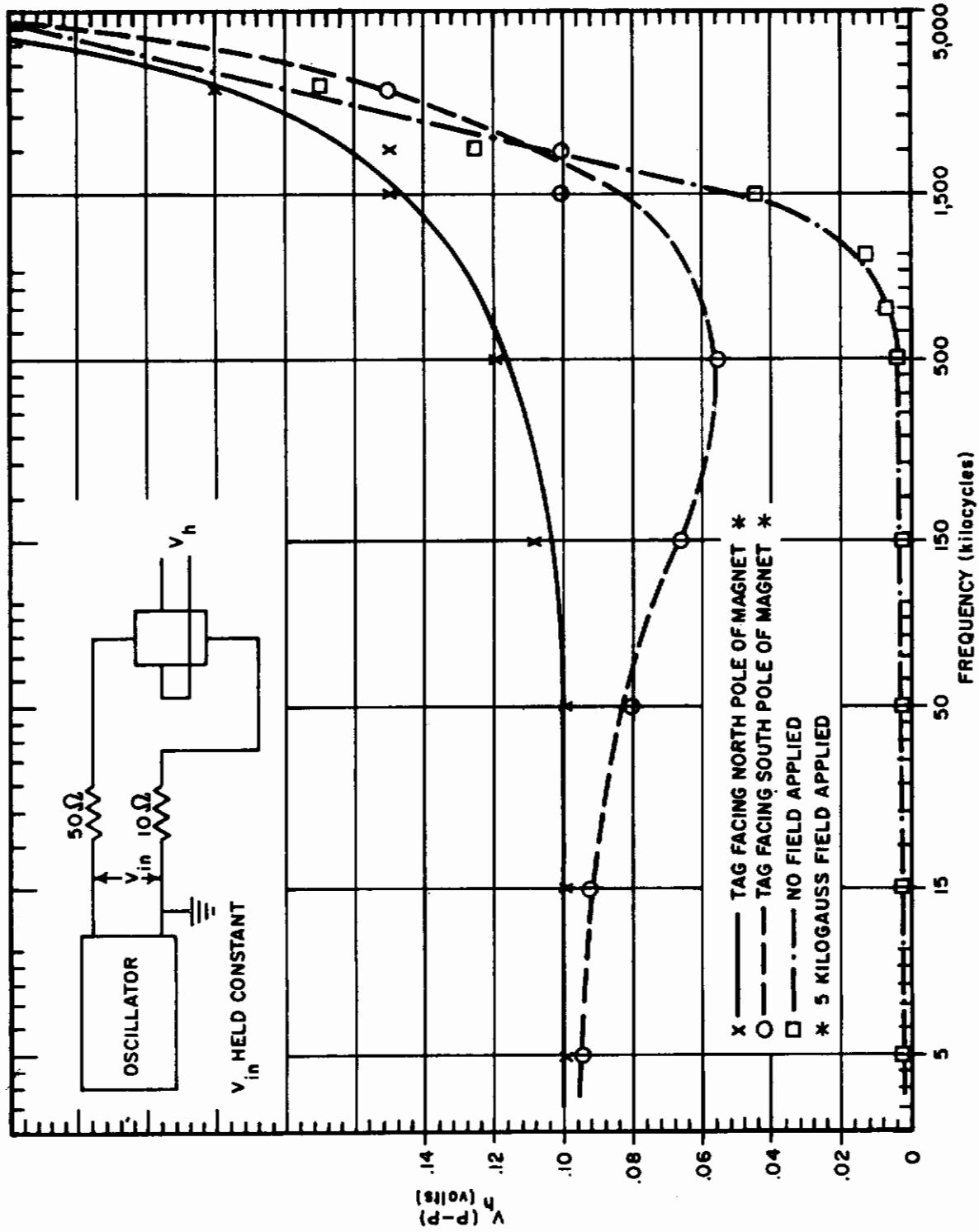

Figure 6. Frequency response of thin-film Hallefex

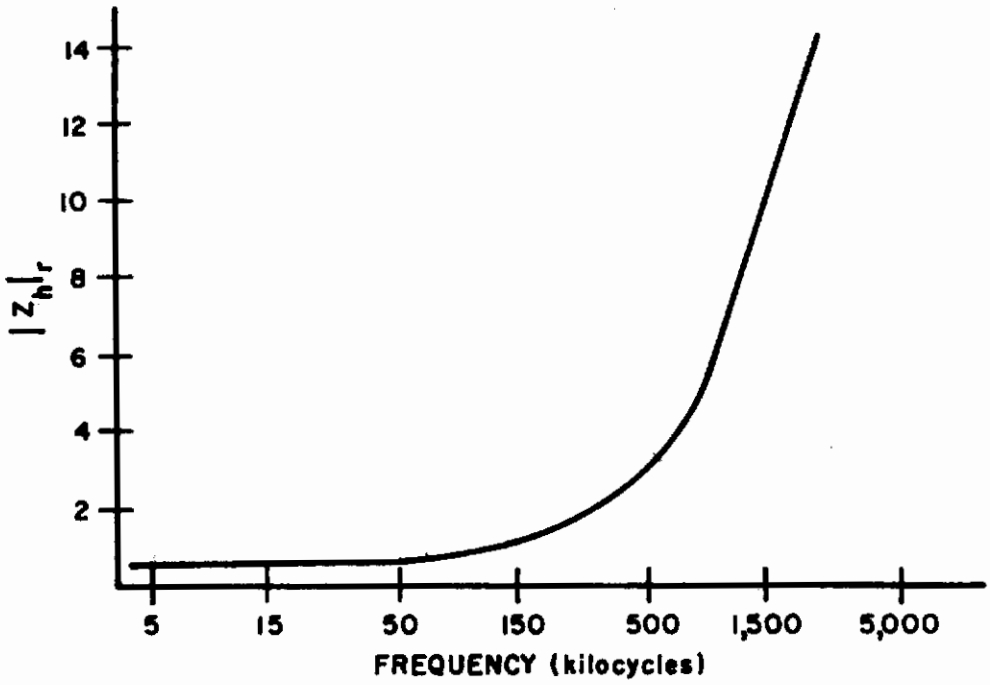

Figure 7. Typical impedance variation with frequency of bulk type

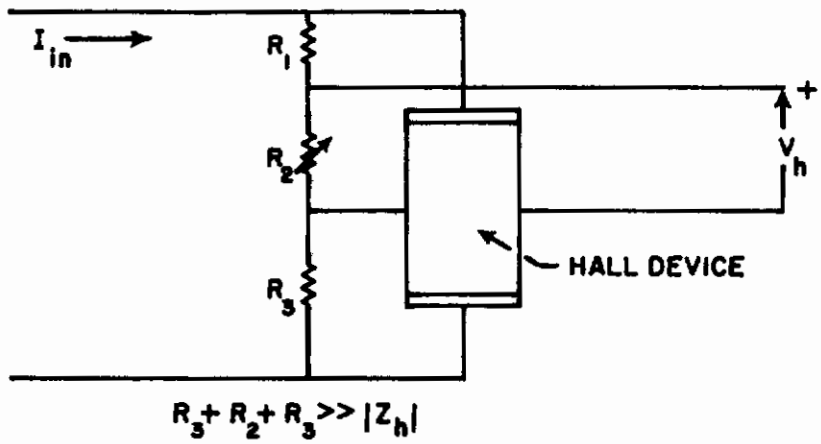

Figure 8. Compensating network

concentrators. By means of concentrators, magnetic fields in the area of 10^{-5} gauss can be measured. The gain of the concentrator would have to be known in order to get the overall sensitivity of the Hall probe.

4. THEORETICAL TRANSIENT RADIATION EFFECTS

a. Gamma and electron irradiation of Hall device materials

The effects discussed here apply primarily to InSb, but much of the same phenomena applies to other semiconductor materials. Thus, for comparing the properties we will include InAs, Ge, and Si.

The effects studied are primarily those caused by gamma radiation, although electrons have been used with Linac experiments, and one test at SPRF with a mixed nuclear environment included neutrons.

Under the heading of TREES (transient radiation effects on electronic systems), there are several effects that may be important, depending on the environment and instrumentation. These are ionizing effects, sudden creation of permanent defects, and the sudden rise of temperature. In many cases these effects are small and there is difficulty in separating them from cable effects and noise. While these small effects are unimportant as far as transient radiation effects on electronic circuits are concerned, it is desirable to understand them and see them clearly enough in experiments so that predictions can be made as to their effects in higher dose rate environments.

In discussing the effect of irradiation on the carrier concentration of a semiconductor, it is essential to specify the Fermi level or the carrier concentration in the sample used.

In figure 9, D is the donor level associated with impurities, and a and d are impurity levels associated with lattice defects. The probability of an energy level's being occupied by an electron, A , depends on the energy as compared to the Fermi level, φ .

The transition of A from unity to zero takes place in an energy range of a few KT around φ, where K is Boltzmann's constant and T is absolute temperature. It can be seen that adding donor levels d below φ

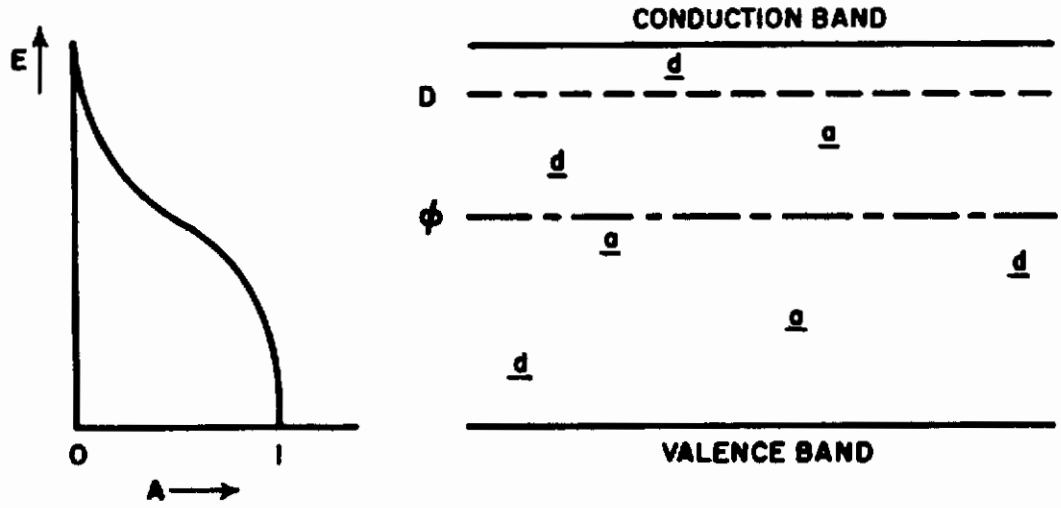

Figure 9. Fermi level diagram

and acceptor levels above φ has no effect on the carrier concentration. But adding acceptor levels below φ reduces the concentration of conduction electrons in n-type material, and adding donor levels above φ increases the concentration. When an electron crosses from the valence band into the conduction band, it produces a free electron in the conduction band and a single hole in the valence band. The absorption by an impurity can produce either an electron in the conduction band or a hole in the valence band.

A negative charge and a positive charge are formed simultaneously when an electron-hole pair is generated. Then both particles can propagate throughout the semiconductor, while at the same time maintaining charge neutrality. Only one of the two freed charges remains mobile in the case of absorption by impurities, the second being fixed to the ionized impurity atom. In such a case, the electron cannot leave the crystal without the condition of charge neutrality being affected unless it is replaced by a new electron entering the crystal from the external circuit. Both cases mentioned result in a change of conductivity during irradiation. Absorption by free carriers or the lattice does not form new carriers.

The generated electrons or holes will have initially high kinetic energies that are soon lost by interaction with the lattice. When the kinetic energy of these particles is large enough, the probability of interaction with the lattice will diminish relative to the probability of collision ionization, which frees a further electron-hole pair. At first, fast electrons are generated in the crystal, and these in turn ionize further atoms. If one assumes that the energy losses of the electron resulting from the electron interacting with the lattice are very small in the high energy region (this is because the mass of the nucleus is much larger than the mass of the electron), the fast electrons should lose only a small amount of energy to the crystal lattice during collisions.

High energy radiation and particles may also result in lattice defects which are formed when atoms are displaced. If an atom is to undergo a displacement, it must acquire a certain minimum energy, which in InSb is 5.7 ev. When this energy is delivered by an electron, it must have an energy of 0.24 Mev. Therefore, gamma rays having energy greater than 0.24 Mev may cause permanent damage to an InSb crystal.* These figures are for liquid nitrogen temperatures. At room temperature almost all defects are annealed out immediately.

The excess electrons and holes temporarily created in a semiconductor by exposure to ionizing radiation enhance the conductivity and Hall constant of the media. The conductivity and Hall constant are a function of the majority carriers. In addition to this current in the volume of the device, there may be an additional current component from surface conduction, or conduction to some other elements of an encapsulating or supporting structure. The degree to which these excess carriers affect the operation of the device will depend on the function of the device. An estimate of the magnitude of the radiation-generated current can be obtained for a device by knowing the geometry and electrical characteristics.

At normal temperatures the generation and recombination processes constantly occur due to the influence of thermal energy. A state of

*F. H. Eisen and P. W. Bickel, Phys. Rev. 115, 345 (1959)

equilibrium is maintained by these processes as determined by Fermi-Dirac statistics. This distribution is independent of the manner in which carriers are either generated or recombined.

The change in carrier density in a semiconductor, δn, can be estimated from the known radiation dose rate, the efficiency of the material in producing carriers (.36 to .72 ev/pair for InSb), and the carrier recombination rate for the material. If the radiation pulse is short compared to carrier lifetime, τ, the total number of excess carriers at the end are proportional to the radiation dose. If the carrier lifetime is much shorter than the radiation pulse, the excess carrier density (δn) at any time during the pulse is

$$\delta n = \delta n_t \, t \tag{31}$$

where t is the time duration of the radiation pulse, and δn_t is obtained from the continuity equation as follows:

$$\left\{\begin{array}{l}\text{Time rate of}\\ \text{increase of}\\ \text{conduction}\\ \text{electrons}\end{array}\right\} = \left\{\begin{array}{l}\text{rate of}\\ \text{generation}\\ \text{of conduction}\\ \text{electrons}\end{array}\right\} - \left\{\begin{array}{l}\text{rate of recom-}\\ \text{bination of}\\ \text{electrons-ion}\\ \text{pairs}\end{array}\right\} \tag{32}$$

$$\delta n_t = g_t - R_t$$

A similar equation also applies to holes. The excess conductivity can be shown to be

$$\delta \sigma = e(\mu_n \delta n + \mu_\rho \delta p) \tag{33}$$

where

μ_n = electron mobility

μ_p = hole mobility

δp = excess number of holes.

Equation (33) reduces to

$$\delta\sigma = \delta n e \mu_n \tag{34}$$

for n-type material where $n >> p$ and $\mu_n >> \mu_p$.

For steady state, $R_t = g_t$, and the steady-state concentration increment is

$$\delta n = g_t \tau \tag{35}$$

where τ = mean lifetime of the carriers. $\tau = 50 \times 10^{-9}$ sec for InSb, and thus equation (35) would apply for InSb when calculating the change in carrier density.

For buildup, we have

$$\delta n = g_t \tau \left[1 - \exp\left(-\frac{t}{\tau}\right)\right] \tag{36}$$

and for decay, we have

$$\delta n = g_t \tau \exp\left(-\frac{t}{\tau}\right) \tag{37}$$

where t is time in seconds.

b. Effects on Hall voltage output

Since current is related to voltage, the increase in the number of carriers calculated by equation (35) will cause a change in conductivity of the material $\delta\sigma$ by the following relation

$$\delta\sigma = e\, \delta n\, \mu \tag{38}$$

Since current is related to the voltage across the device by the relation

$$i = \sigma V wd/\ell \tag{39}$$

the change in current through the device will then be

$$\delta i = \delta\sigma\ V wd/\ell \tag{40}$$

The change in Hall voltage output, δV_h, may be calculated for three different modes of operation, assuming the conventional Hall voltage equation holds under the radiation conditions. This relationship was shown by equation (15) and is repeated for convenience:

$$V_h = \frac{R_h B I}{d} \tag{41}$$

The three cases considered are for the Hall device operated with the bias circuit as a

(1) constant voltage source,

(2) constant current source,

(3) constant power source.

(1) Constant voltage source

This circuit arrangement is shown in figure 10.

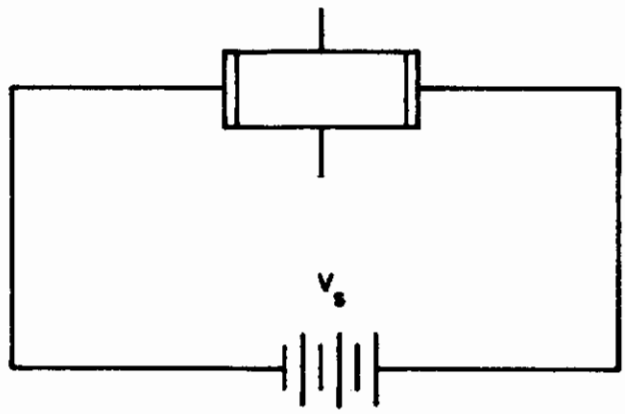

Figure 10. Constant voltage source bias circuit

By using the relations for the Hall coefficient and current density in the Hall voltage equation, we get the following results:

$$R_h = \frac{1}{ne} \tag{42}$$

where

n = number of conduction electrons

e = charge of an electron

and

$$\frac{I}{dw} = \frac{en\mu V_s}{\ell} \tag{43}$$

$$I = en\mu \frac{wd}{\ell} V_s$$

where

μ = mobility

V_s = source voltage

d, w, and ℓ = dimensions of sample as shown in figure 2.

Then

$$V_h = \frac{R_h B I}{d} \tag{44}$$

$$V_h = \frac{B \mu w}{\ell} V_s \tag{45}$$

Equation (45) indicates that for a constant voltage source the Hall voltage should remain constant during a radiation pulse, since B, μ, V_s and the device's dimensions are not a function of the radiation energy absorbed.

(2) Constant current source

The constant current source has a large output impedance compared to the Hall device input impedance. This circuit arrangement (figure 11) keeps the current through the device constant.

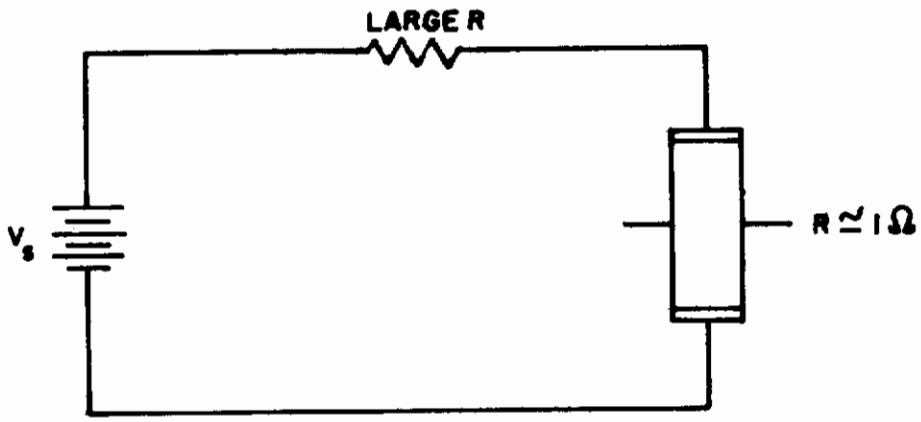

Figure 11. Constant current source bias circuit

Then using equations (41) and (42) we obtain

$$V_h = \frac{B\,I}{ned} \tag{46}$$

The current in the Hall voltage equation will be a constant. Then if n changes by an amount δn, we define a quantity δV_h, the change in Háll voltage, by

$$V_h + \delta V_h = \frac{K_1}{n + \delta n} \tag{47}$$

where $K_1 = \frac{BI}{ed}$,

so that

$$\delta V_h = \frac{K_1}{n + \delta n} - \frac{K_1}{n} \tag{48}$$

(3) Constant power source

If energy is supplied to the Hall device at a constant rate, we obtain the result that Hall voltage is a function of $\frac{1}{\sqrt{n}}$ in the following

manner. The power equation is

$$P = I^2 R \tag{49}$$

The resistance, R, can be expressed in terms of the resistivity and dimensions of the device by

$$R = \frac{\rho \ell}{wd} \tag{50}$$

Then

$$I = \left(\frac{Pwd}{\rho \ell}\right)^{1/2} \tag{51}$$

Next, using equation (50) and the following relations for R_h and ρ in the Hall voltage equation we obtain

$$R_h = \mu \rho, \text{ and } \rho = \frac{1}{ne\mu} \tag{52}$$

$$V_h = \left(\frac{\mu}{n}\right)^{1/2} B \left(\frac{Pw}{e \ell d}\right)^{1/2} \tag{53}$$

$$V_h = \frac{K_2}{\sqrt{n}} \qquad \text{when } K_2 = B \left(\frac{P \mu w}{e \ell d}\right)^{1/2} \tag{54}$$

If n changes by an amount δn, the change in Hall voltage, δV_h, will be given by

$$V_h + \delta V_h = \frac{K_2}{\sqrt{n + \delta n}} \tag{55}$$

so that

$$\delta V_h = \frac{K_2}{\sqrt{n + \delta n}} - \frac{K_2}{\sqrt{n}} \tag{56}$$

Equations (48) and (56) indicate that the Hall voltage should decrease when n-type material is irradiated by gamma rays.

The assumption is made that the number of holes generated during a radiation pulse will be equal to or less than the number of electrons. If this assumption is not good, we will have to use the more complicated expression for Hall voltage given by combining equations (15) and (24),

$$V_h = \frac{BI}{d} \frac{3\pi}{8e} \frac{-n\mu_n^2 + p\mu_p^2}{(e\mu_n n + e\mu_p p)^2} \tag{57}$$

c. Variation of the Hall coefficient with change of the ratio of electrons to holes

From table 1 it can be seen that the holes are much less mobile than electrons for InSb. When such materials are intrinsic, the Hall coefficient and resistivity are determined almost entirely by electrons. Even for p-type material the Hall coefficient will be negative when there are several times more holes than electrons. From equation (25) we have

$$R_h = \frac{\frac{3\pi}{8}}{n_i e} \frac{(1 - b\,c)\sqrt{c}}{(1 + b\,c)^2} \tag{58}$$

where n_i = intrinsic carrier concentration,

$b = \mu_n/\mu_p$, and

$c = \dfrac{\text{electron concentration}}{\text{hole concentration}}$

Consider now the behavior of R_h as c varies from infinity to zero, n_i remaining constant. This equation is plotted in figure 12. It is an indication of how the electrical properties of a semiconductor change as the ratio of electrons to holes change as a consequence of a large mobility ratio. This plot is somewhat idealized because μ and b are themselves functions of c. But it does show that for n-type material the Hall coefficient (R_h) changes slowly as a function of c, whereas for p-type material the change could be quite large. It also indicates that for large radiation doses when the change in carrier concentration approaches 10^{16}, R_h will have increased

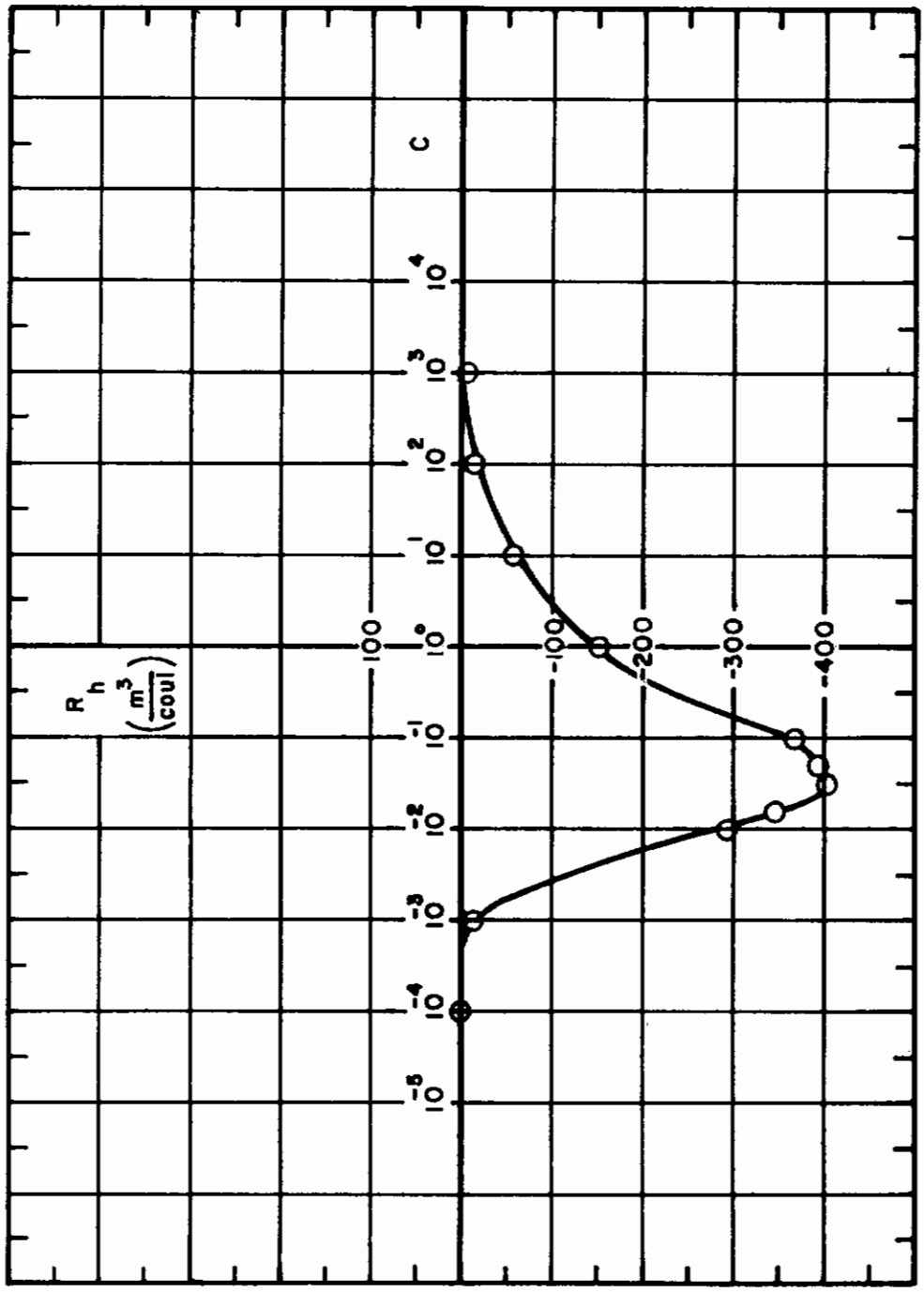

Figure 12. Plot of R_h vs. c

about 8 times. Thus the interpretation of Hall coefficient will not always be simple.

An ionizing radiation which changes the majority carrier concentration by a negligibly small amount may enhance the minority carrier concentration by orders of magnitude.

d. Procedure for calculating the transient radiation effects on the Hall device when irradiated with gamma ray systems

(1) Obtain the data on dose and dose rate of irradiating gamma beams at the location of the experiment. These data should be expressed in ergs/cm^2 and ergs/cm^2/sec, and will be designated I_o and I_o/sec.

(2) Obtain the absorption coefficients (μ_a) for InSb. For a good approximation we can use the μ_a for tin, because tin has approximately the same density and atomic weight as indium antimonide. These values are shown in table 2. The μ_a for tin were obtained from Fundamental Aspects of Reactor Shielding.*

(3) Calculate the total energy absorbed in ev by the formula:

$$\Sigma_{abs} = \mu_a \frac{cm^2}{gram} \cdot I_o \frac{ergs}{cm^2} \cdot \frac{gram}{device} \cdot \frac{10^7 \text{ ev}}{1.6 \times 10^{-19} \text{ ergs}} \quad (59)$$

(4) For gamma irradiations almost all of the energy of the incident gamma rays is converted into electrons by photoelectric and Compton events. In silicon and germanium, the ionization efficiency appears to be between 3 and 4 ev per electron-ion pair. The energy lost per electron ionized in any material can be approximated as 2 to 4 times the ionization potential of the material. These are the figures commonly used in the literature. This ionization potential in solid-state materials is interpreted to be the forbidden energy gap, which is 0.18 ev for InSb. The ionizing efficiency for InSb is then about 0.36 to 0.72 ev per electron-ion pair.

*H. Goldstein, Addison-Wesley, 1959, p. 237, tables 5-10

Table 2

ABSORPTION COEFFICIENTS FOR InSb

Mev	μ_a	Mev	μ_a
0.3	.0876	6.0	.0293
0.4	.0536	9.0	.0321
0.5	.0401	10.0	.0345
0.6	.0346	15.0	.0401
0.8	.0294	20.0	.0445
1.0	..0268	30.0	.0507
1.5	.0239	40.0	.0549
2.0	.0234	50.0	.0583
3.0	.0243	60.0	.0611
4.0	.0260	80.0	.0648
5.0	.0278	100.0	.0677

To obtain the number of carriers produced, the following formula may be used:

$$n_s = \frac{\text{energy absorbed (ev)}}{0.36 \text{ ev/electron-ion pair}} \qquad (60)$$

Assuming a square wave radiation pulse of 0.2×10^{-6} second duration, the rate $\left[g_{(t)}\right]$ of the generation of conduction electrons is given by:

$$g_t = \frac{n_s}{t} = \frac{n_s}{2} \times 10^7 \text{ electrons/sec} \qquad (61)$$

From here on the procedure is given by equations (31) through (58).

e. Calculation of change in Hall voltage for constant current operation

These calculations are based on the following assumption of operating conditions of the Hall device and the dose rate.

Room temperature

$N = 4 \times 10^{16}$ electrons/cm^3 at room temperature

Average energy 1 Mev

μ_a absorption coefficient = 0.0268

Pulse length 10 μsec

HS-51 Halltron biased at 300 ma DC and mounted at 45° to magnetic field and radiation

Magnetic field 1 kilogauss

0.05 gram InSb/device

The equation for the change in Hall voltage for constant current operation was given by equation (48) as

$$\delta V_h = \frac{K_1}{n + \delta n} - \frac{K_1}{n}$$

The constant K_1 can be determined experimentally for the particular experiment by measuring the Hall voltage. For the above conditions, $V_h = 30 \times 10^{-3}$ volt. This allows one to calculate the constant K_1 from the Hall voltage equation.

$$V_h = \frac{BIR_h}{d} = \frac{K_1}{n} \qquad (62)$$

Then

$$K_1 = n V_h = 1.2 \times 10^{15}$$

Next, we want to get δn as a function of dose rate. This will then allow one to calculate the values of δV_h as a function of dose rate. These data are tabulated in table 3.

Table 3

PERCENT CHANGE IN HALL VOLTAGE
AS A FUNCTION OF DOSE RATE

$\dot{D}$ r/sec	ΔV_h(%)
10^8	9.1×10^{-8}
10^9	.01
10^{10}	9
10^{11}	50
10^{12}	90
10^{13}	99

From equations (60) and (61) we have

$$g_t = \frac{\mu_a \left(\frac{cm^2}{gram}\right) \cdot ev/cm^2/sec \cdot 2\ gram/device}{0.36\ ev} \left(\frac{electron}{sec}\right) \quad (63)$$

To convert from r/sec to $ev/cm^2/sec$, we use a curve from the Radiological Health Handbook. *

1 r/hour = 6×10^5 Mev/cm^2-sec at 1-Mev energy

*U. S. Department of Health, Education and Welfare, PB121784, p. 140

In terms of $ev/cm^2/sec$ this is equivalent to

$$2.16 \times 10^{15} \text{ ev/cm}^2 \text{ r} \times \text{dose rate in r/sec}$$

Equation (63) then becomes

$$g_t = 8.04 \times 10^{12} \dot{D} \text{ electrons/sec} \tag{64}$$

where

$\mu_a = 0.0268$

$ev/cm^2/sec = 2.16 \times 10^{15}$

$\dot{D}$ = dose rate in r/sec

$\frac{\text{gram}}{\text{device}} = 0.05$

Next we make use of equation (35) to get δn, remembering that $\tau = 50 \times 10^{-9}$ sec. Equation (35) reads

$$\delta n = g_t \tau$$

so that

$$\delta n = 4.02 \times 10^{5} \dot{D} \text{ electrons} \tag{65}$$

From equation (48), we get δV_h, the change in Hall voltage, as a function of dose rate. It is

$$\delta V_h = \frac{K_1}{n + \delta n} - \frac{K_1}{n}$$

Inserting the values for K, n, and δn, we have

$$\delta V_h = \frac{12 \times 10^{14}}{4 \times 10^{16} + 4.02 \times 10^{5} \dot{D}} - .03 \tag{66}$$

The values of δV_h given in table 3 were obtained from equation (66). They are somewhat idealized in that recombination rate and δp, the change in

hole concentration, may also be a function of energy absorbed. It is reasonable to assume, especially for materials not having a direct recombination process, that the values for percent change in Hall voltage are within two orders of magnitude.

f. Effects on displacement voltage

The displacement voltage of a Hall device is a voltage drop due to the bias current as explained in section 3d. The transient radiation effect will not be calculated. The resistance is obtained from the formula

$$R = \frac{\rho \ell}{A} \tag{67}$$

where

ρ = resistivity
ℓ = length of sample
A = cross section area

Then using the relation for the resistivity ρ, given by

$$\rho = \frac{1}{ne\mu} \tag{68}$$

and assuming the mobility remains constant during irradiation, the change in resistance, δR, is obtained as

$$\delta R = \frac{\ell/A}{(n + \delta n)e\mu} - \frac{\ell/A}{ne\mu} \tag{69}$$

The change in displacement voltage as monitored across the Hall voltage leads can then be calculated for constant current bias. It is

$$\delta V_d = i\delta R = \frac{K}{n + \delta n} - \frac{K}{n} \tag{70}$$

For the condition of constant voltage bias there would be no change in Hall voltage, because the voltage drop across the device is constant. The displacement voltage transient radiation effects change in the same manner as Hall voltage for the same operating conditions.

5. EXPERIMENTAL TRANSIENT RADIATION EFFECTS

a. Experiments using the flash X ray

The AFWL 600-kv flash X-ray system has a radiation output pulse which is approximately a square wave of 0.2-microsecond duration. To see a radiation effect, the irradiated device should have a frequency response which is flat from DC to 2.5 megacycles. The theory predicts that any change in Hall voltage should follow the shape of the radiation pulse for InSb. Since the bulk-type devices have an upper cutoff frequency of about 150 kc, any signal generated due to transient radiation effects would probably be lost. The thin-film device has a much better frequency response, but no effects were observed above the noise level for constant voltage or constant current bias. The circuits used are similar to that used for the Linac experiments described in the next section.

b. Experiments on the WSMR gamma Linac

Pulse widths of 10 microseconds were used; thus, any generated transient radiation effects should have been observed on any of the Hall devices used.

The physical arrangement of the Hall device in relation to the Linac and magnet are shown in figure 13. The Hall device is located at an angle of 45° to both the magnetic field and the gamma ray beam. The magnetic field strength was about 1.5 kilogauss. A copper shield enclosed the whole system in the radiation room. This was to reduce RF noise pickup. There was an aluminum foil window in the copper shield for the radiation beam to pass through. The apparatus is shown in figures 14 and 15.

The circuit arrangements for observing changes in Hall voltage and bias current are shown in figures 16 and 17. The waveforms were

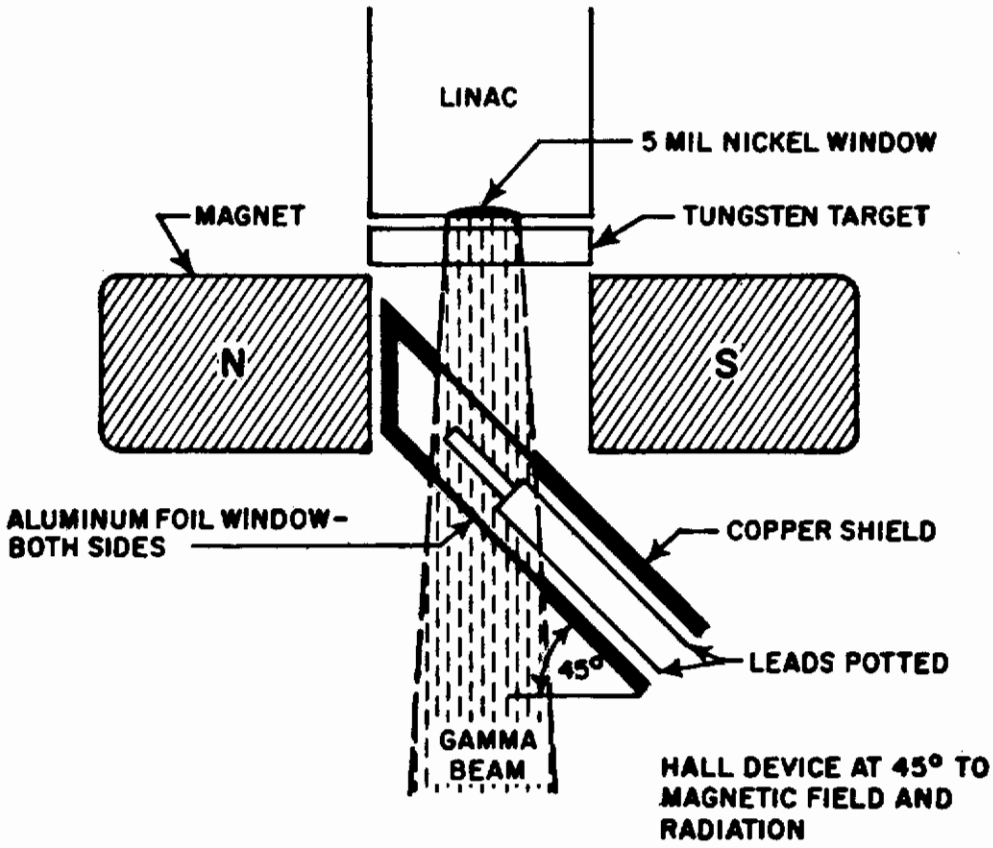

Figure 13. Physical arrangement for Hall voltage in relation to the magnetic field and radiation beam

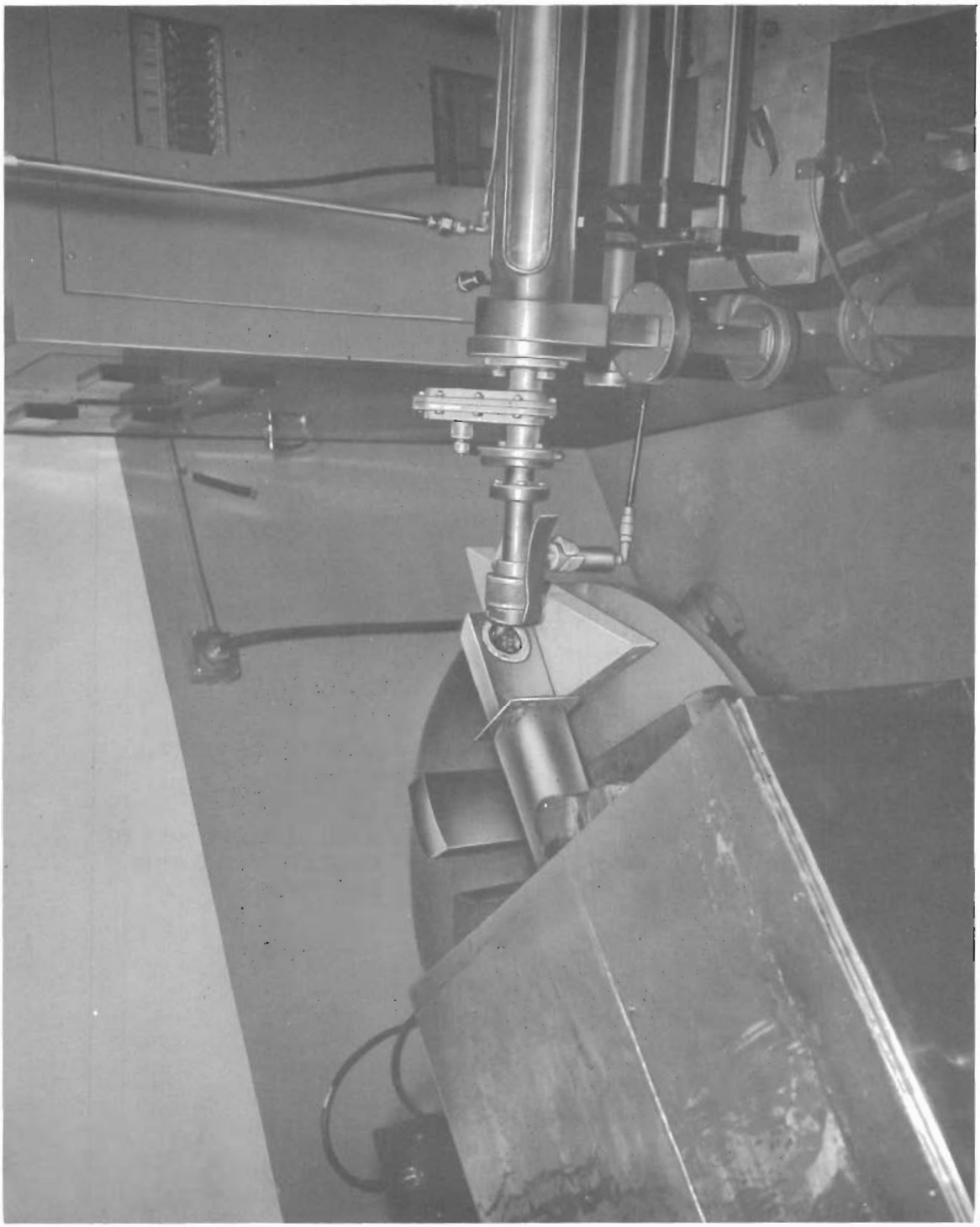

Figure 14. Copper shielding in place by Linac

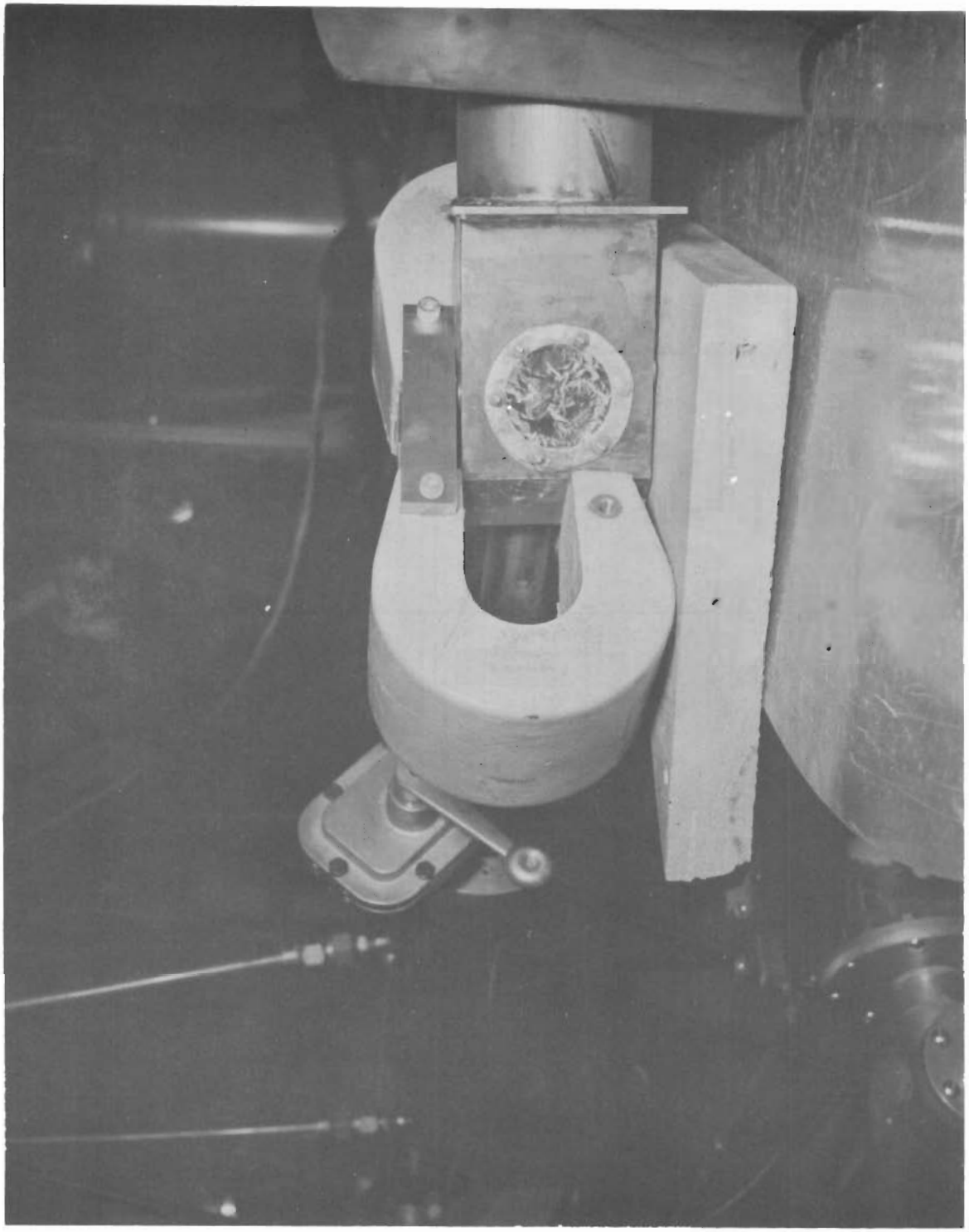

Figure 15. Magnet and apparatus in test position

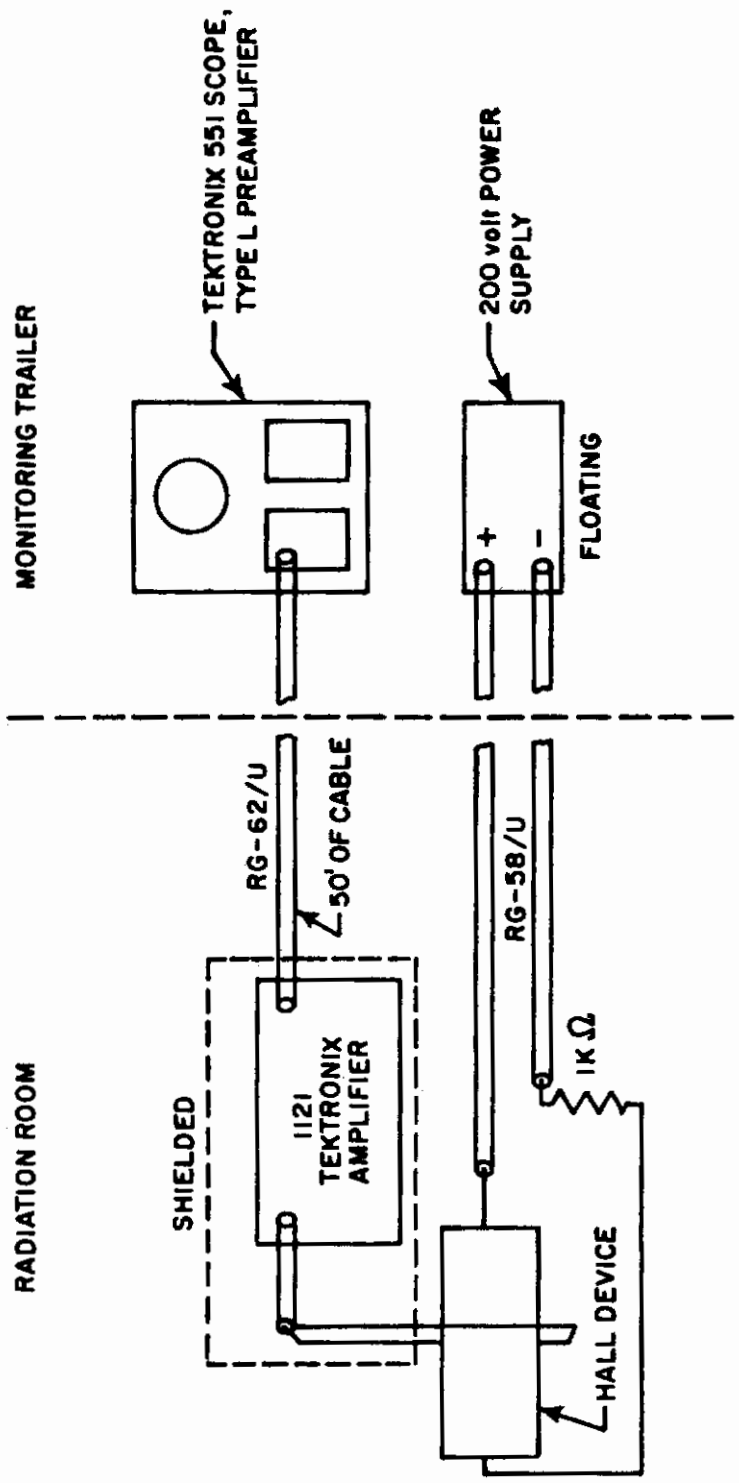

Figure 16. Experimental arrangement for Hall voltage measurement with constant current bias on the Hall device

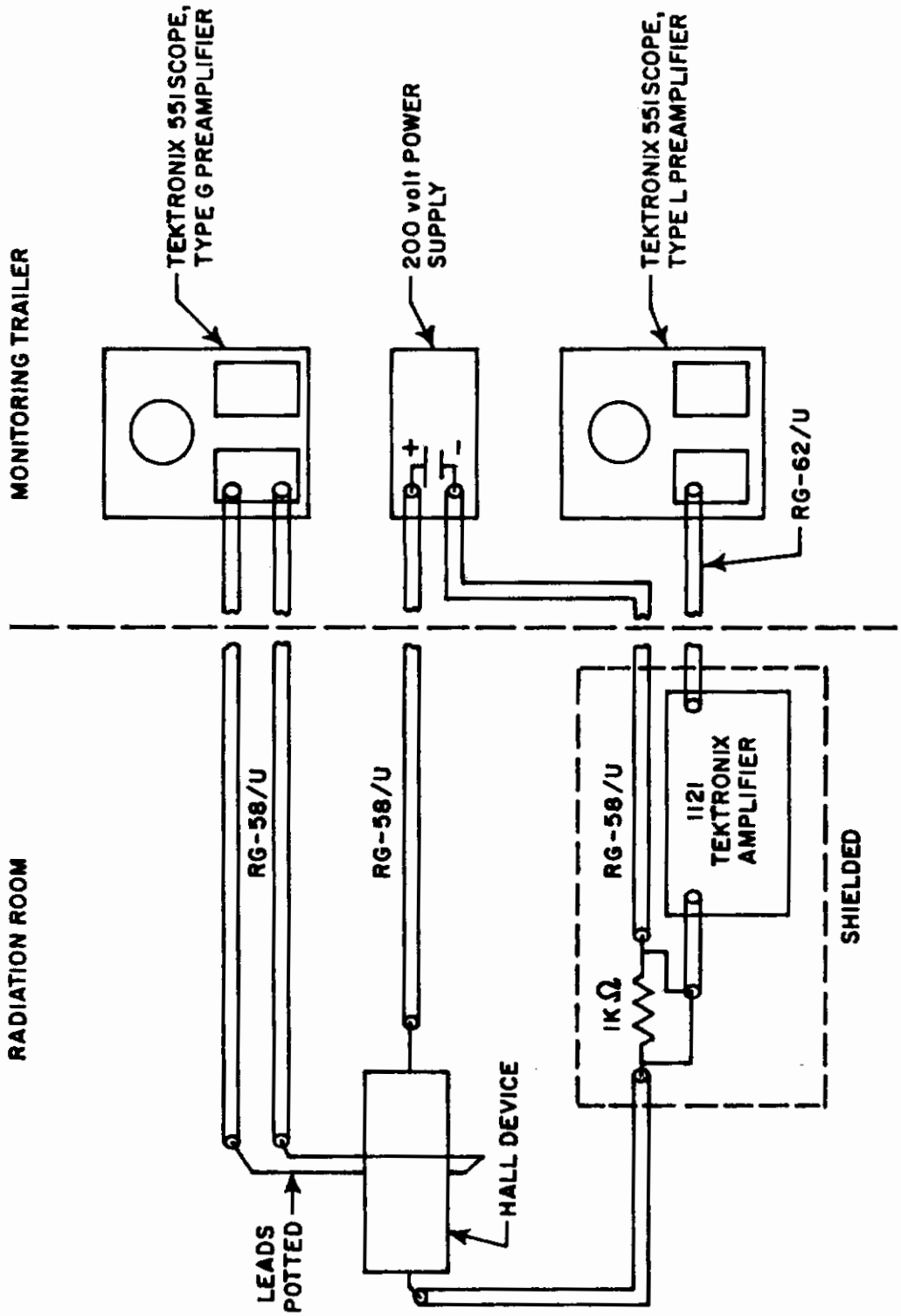

Figure 17. Monitoring system for measuring ΔI

observed by using Polaroid cameras on the oscilloscopes. Lead shielding was used around the amplifier in the radiation room. The system was capable of measuring changes as low as 10 microvolts, which is below the noise level when the Linac is pulsed. The gamma dose rate obtained was between 10^5 and 10^6 r/sec.

From the results of the Linac experiments no clear picture of transient radiation effects could be observed for Hall voltage change using a constant current bias. The effects due to back-scattered gamma radiation and RF pickup in cables and the amplifier were minimized by the use of lead and copper shielding. The liquid nitrogen experiments had similar results.

Figure 18 is a picture of the electron beam pulse shape in the Linac. For comparison, figure 19 is a picture of the gamma radiation pulse as monitored by a pilot B crystal and photodiode.

6. CORRELATION OF EXPERIMENTAL AND THEORETICAL DATA

Since no clear transient radiation effects were observed experimentally for dose rates up to 10^7 r/sec, the experiments back up the theory for dose rates less than 10^7 r/sec.

To further prove the theory for semiconductors, larger dose raté machines will be required.

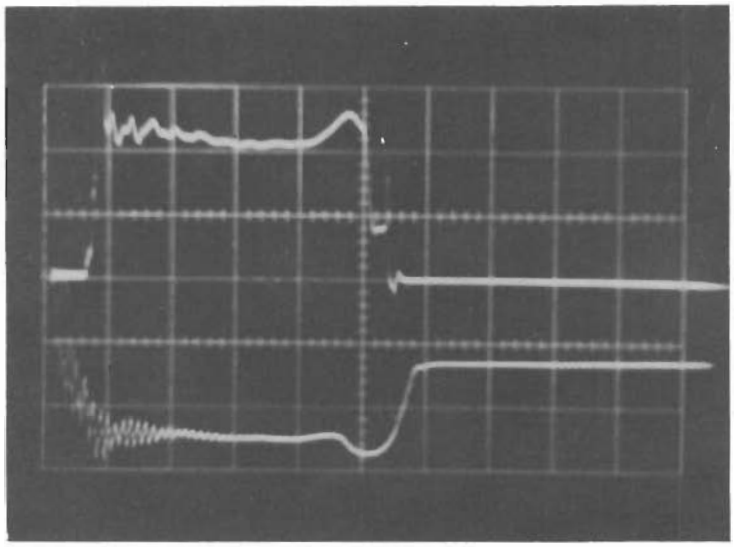

Figure 18. Linac electron beam pulse as measured by the wire loop method
Amplitude is 0.5 V/cm, and time base 2 μsec/cm

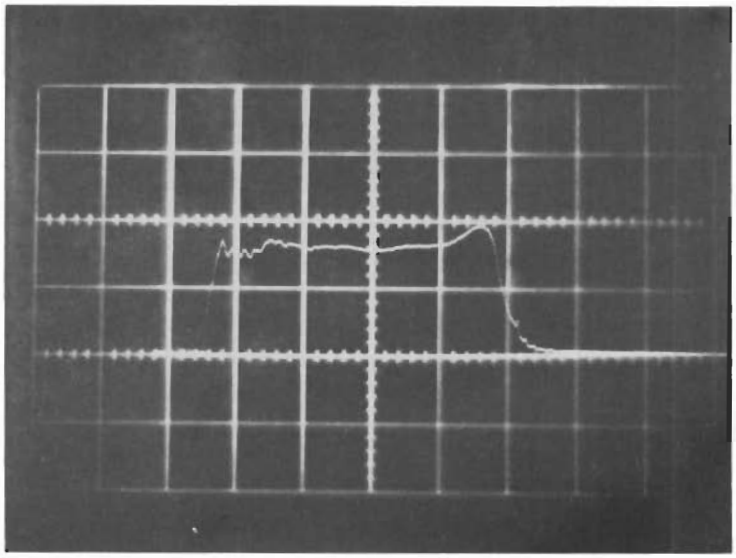

Figure 19. Linac gamma radiation pulse as measured by pilot B crystal and photodiodes
Time base is 2 μsec/cm

DISTRIBUTION

No. cys

HEADQUARTERS USAF

1 Hq USAF (AFCOA), Wash, DC 20330
1 Hq USAF (AFDED), Wash, DC 20330
1 Hq USAF (AFNIN), Wash, DC 20330
1 Hq USAF (AFORQ), Wash, DC 20330
1 Hq USAF (AFRDC/NE), Wash, DC 20330
1 Hq USAF (AFRDP), Wash, DC 20330
1 Hq USAF (AFRNE-A), Wash, DC 20330
1 Hq USAF (AFRNE-B), Wash, DC 20330
1 Hq USAF (AFRST), Wash, DC 20330
1 Hq USAF (AFTAC), Wash, DC 20330

MAJOR AIR COMMANDS

1 ADC (ADLPD), Ent AFB, Colorado Springs, Colo 80912
1 AFLC (MCSW), Wright-Patterson AFB, Ohio 45433
1 AFSC (SCT), Andrews AFB, Wash, DC 20331
1 AUL, Maxwell AFB, Ala 36112

SAC, Offutt AFB, Nebr 68113
1 (OA)
1 (DICC)
1 (DPLBC)

TAC, Langley AFB, Va 23365
1 (TPL-RWD-M)
1 (DORQ-M)

1 USAFIT, Wright-Patterson AFB, Ohio 45433
1 USAFA, Colo 80840

AFSC ORGANIZATIONS

ASD, Wright-Patterson AFB, Ohio 45433
1 (SEPIR)
1 (ASZGDW)
1 (ASAPR)

DISTRIBUTION (cont'd)

No. cys	
	ESD, Hanscom Fld, Bedford, Mass
2	(ESTI)
1	(ESAT)
	BSD, Norton AFB, Calif 92409
1	(BST)
1	(BSQ)
5	(BSRGA)
	FTD, Wright-Patterson AFB, Ohio 45433
1	(TDBTL)
1	(TD-BI)
1	RTD (RTN-W, Lt Col E. D. Munyon)
1	RTD (RTSUM), 68 Albany St, Cambridge 39, Mass
1	RTD (SENPO, Mr. P. E. Gray), Wright-Patterson AFB, Ohio 45433
	SSD, AF Unit Post Office, Los Angeles, Calif 90045
1	(SSSD)
1	(SSZM, Lt Col T. O. Wear)
1	(SSTRS, Maj D. L. Evans)
1	(SSTRT, Capt J. Van Dusen)
1	(SSTDS, Lt V. Bouquet)
1	AFMTC (MU-135, Tech Library), Patrick AFB, Fla 32925
1	APGC (PGBAP-1), Eglin AFB, Fla 32542
	RADC, Griffiss AFB, NY 13442
1	(Mr. D. Benson)
1	(EMERM)
1	(EMEAM)
1	(EML, Library)
1	(RASGP, Mr. D. Kenneally)
1	6593 Test Group (Development), Edwards AFB, Calif 93523
1	AF Avionics Laboratory, Wright-Patterson AFB, Ohio 45433
1	AF Materials Laboratory, Wright-Patterson AFB, Ohio 45433
1	AF Msl Dev Cen (RRRT), Holloman AFB, NM 88330

DISTRIBUTION (cont'd)

No. cys	
	KIRTLAND AFB ORGANIZATIONS
	AFSWC, Kirtland AFB, NM 87117
1	(SWEH)
1	(SWTT)
	AFWL, Kirtland AFB, NM 87117
20	(WLIL)
1	(WLR)
1	(WLRJ)
1	(WLRPE)
1	(WLRM)
1	(WLA)
1	(WLD)
1	(WLX)
1	(WLF)
1	(WLRPC)
20	(WLDN-1)
1	ADC (ADSWO), Special Weapons Office, Kirtland AFB, NM 87117
	OTHER AIR FORCE AGENCIES
2	Director, USAF Project RAND, via: Air Force Liaison Office, The RAND Corporation, ATTN: Mr. J. Whitener, 1700 Main Street, Santa Monica, Calif 90406
1	AFCRL, Hanscom Fld, Bedford, Mass 01731
1	AFOAR (RRN), Bldg T-D, Wash, DC 20333
1	AFOSR (SREC), Bldg T-D, Wash, DC 20333
	ARMY ACTIVITIES
	Chief of Research and Development, Department of the Army, Wash, DC 20310
1	(Special Weapons and Air Defense Division)
1	(Atomic Division, Lt Col D. Baker)
3	US Army Material Command, Harry Diamond Laboratories (ORDTL 06.33, Technical Library, and Chief, Nuclear Vulnerability Branch, 230), Wash, DC 20438

DISTRIBUTION (cont'd)

No. cys

1	Commanding General, US Army Materiel Command, ATTN: AMCRD-DE-N, Wash, DC 20315
1	Commanding Officer, US Army Combat Developments Command, Nuclear Group (USAGDCNG), ATTN: Maj Doerflinger, Ft Bliss, Tex 79916
3	Redstone Scientific Information Center, US Army Missile Command, Chief, Document Section, Redstone Arsenal, Ala 35809
1	Director, Ballistic Research Laboratories (Library), Aberdeen Proving Ground, Md 21005
	Commanding General, Picatinny Arsenal, Dover, NJ 07801
1	(SMUPA-VC1, R. Kesselman)
1	(SMVPA-VA6, Samuel Feltman Ammunition Laboratories)
3	Commanding Officer, Electronics Research and Development Laboratory (AMSELRALNA and AMSELRAXS), Ft Monmouth, NJ 07703
2	Commanding General, White Sands Missile Range (Tech Library, STEWS-AMTED-E, Mr. Glenn Elder), White Sands, NM 88002

NAVY ACTIVITIES

	Office of the Chief of Naval Operations, Department of the Navy, Wash, DC 20350
1	(OP-36)
1	(OP-754)
	Chief, Bureau of Naval Weapons, Department of the Navy, Wash 25, DC
1	(RMGA-8)
1	(RRNV)
1	Chief, Bureau of Ships, Department of the Navy (Code 362B), Wash, DC 20360
1	Commanding Officer, Naval Research Laboratory, Wash, DC 20390
1	Commanding Officer and Director, US Naval Radiological Defense Laboratory, San Francisco, Calif 94135
1	Commanding Officer and Director, Navy Electronics Laboratory (Code 4223), San Diego, Calif 92152
1	Commanding Officer, Naval Aviation Materiel Center, Philadelphia, Pa

DISTRIBUTION (cont'd)

No. cys

1 Commanding Officer, Naval Air Development Center, Johnsville, Pa

1 US Naval Avionics Facility, 21st and Arlington Ave, Indianapolis, Ind

1 Commanding Officer and Director, Naval Applied Science Laboratory, Brooklyn 1, NY

1 Commander, Naval Ordnance Laboratory, ATTN: Dr. Rudlin, White Oak, Silver Springs, Md 20390

Office of Naval Research, Wash 25, DC

1 (Code 418)

1 (Code 427)

1 Commanding Officer, US Naval Weapons Evaluation Facility (NWEF) (Code 404), Kirtland AFB, NM 87117

1 Commanding Officer, Naval Ordnance Laboratory, ATTN: Dr. Bryant, Corona, Calif

OTHER DOD ACTIVITIES

Director, Defense Atomic Support Agency, Wash, DC 20301

1 (Document Library Branch)

1 (DASARA-4, Maj P. K. Mitchell)

Commander, Field Command, Defense Atomic Support Agency, Sandia Base, NM 87115

1 (FCAG3, Special Weapons Publication Dist)

1 (FCTG)

1 (FCWT)

1 Director, Defense Intelligence Agency, ATTN: DIAAP-1K2, Wash, DC 22212

1 Director, Weapon Systems Evaluation Group, Rm 1D-847, The Pentagon, Wash, DC 20330

1 Director, Advanced Research Projects Agency, The Department of Defense, ATTN: Maj G. G. Sherwood, The Pentagon, Wash, DC 20301

1 Military Secretary, Joint Chiefs of Staff, Director, Communications-Electronics, J6, Wash, DC 20330

20 Hq Defense Documentation Center for Scientific and Technical Information (DDC), Bldg 5, Cameron Sta, Alexandria, Va 22314

DISTRIBUTION (cont'd)

No. cys

AEC ACTIVITIES

No. cys	
1	US Atomic Energy Commission (Headquarters Library, Reports Section), Mail Section G-017, Wash, DC 20545
	Sandia Corporation, Box 5800, Sandia Base, NM 87115
1	(Information Distribution Division)
1	(Dr. J. W. Easley, Dept 5300)
1	(Dr. C. D. Broyles, Dept 5113)
1	(S. C. Rogers, Dept 5312)
1	(A. W. Snyder, Dept 5313)
1	(F. A. Gross, Dept 9130)
2	University of California, Lawrence Radiation Laboratory (Technical Information Division), P. O. Box 808, Livermore, Calif 94551
	Director, Los Alamos Scientific Laboratory, P. O. Box 1663, Los Alamos, NM 87554
1	(Helen Redman, Report Library)
1	(Dr. J. Malik)
2	Brookhaven National Laboratory, ATTN: Dr. C. H. Vineyard, Upton, Long Island, NY
2	Oak Ridge National Laboratory (Tech Library), Oak Ridge, Tenn 37831
2	Argonne National Laboratory (Tech Library), 9700 Cass Ave, Argonne, Ill 60440

OTHER

1	Assistant to Secretary of Defense for Atomic Energy, Wash, DC 20330
1	Central Intelligence Agency (OCR), 2430 E Street NW, Wash, DC 20505
1	OTS, Department of Commerce, Wash 25, DC
6	Institute for Defense Analysis, Rm 2B257, The Pentagon, Wash 25, DC THRU: ARPA
3	Aerospace Corporation, ATTN: Mr. J. Statsinger, P. O. Box 95085, Los Angeles 45, Calif
2	Aerospace Corporation, ATTN: J. Beneveniste, San Bernardino, Calif

DISTRIBUTION (cont'd)

No. cys	
1	AC Spark Plug Company, Dept 32, Milwaukee 1, Wisc 53201
1	Admiral Corporation, ATTN: Mr. R. Whitener, 3800 Cortland Street, Chicago 47, Ill
1	Aerojet-General Corporation, ATTN: B. J. Gastineau, 6352 Irwindale Avenue, Azusa, Calif
1	American Components, Inc., ATTN: Mr. Wellard, 8th Ave at Harry Street, Conshohocken, Pa
1	ARINC Research Corporation, ATTN: Mr. W. Schultz, 1700 K Street NW, Wash 6, DC
1	ARMA Division, American Bosch Arma Corporation, Garden City, Long Island, NY
1	Atomics International, ATTN: W. E. Perkins, Mgr Research, 8900 Desoto Street, Canoga Park, Calif
2	Autonetics Division, North American Aviation, Inc., ATTN: Mr. Albert Lucic, D-3342-4, Bldg 22, Anaheim, Calif
2	AVCO Mfg Corporation, Research & Advanced Development Div., ATTN: J. J. Mayo, 201 Lowell Street, Wilmington, Mass
2	Bell Telephone Laboratories, Inc., Whippany Road, Whippany, NJ
15	The Boeing Company, Aero-Space Division, ATTN: Dr. Glen L. Keister, Org 2-5470, P. O. Box 3707, Seattle 24, Wash
1	Burroughs Corporation, Central Ave and Route 202, Paoli, Pa
1	DASA Data Center, General Electric TEMPO, 735 State Street, Santa Barbara, Calif
1	Director, Applied Physics Laboratory, Johns Hopkins University, ATTN: Mr. Robert Frieberg, 8621 Georgia Ave, Silver Springs, Md
1	Douglas Aircraft Co, Inc., Missile & Space Systems Div, ATTN: Dr. Benjamin Barnett, 3000 Ocean Park Blvd, Santa Monica, Calif
10	General Atomic Division, General Dynamics Corporation, ATTN: Dr. V. A. J. van Lint, P. O. Box S, Old San Diego Station, San Diego, Calif 92110
2	General Dynamics/Fort Worth, ATTN: W. E. Rose, Fort Worth, Tex
1	General Electric Co, Radiation Effects Operations, Defense Systems Dept, ATTN: Mr. L. Dee, 300 South Geddes St, Syracuse, NY
1	General Electric Co, Power Tube Dept, Bldg 269, ATTN: Mr. David Hodges, 1 River Road, Schenectady, NY
1	General Electric Co, Receiving Tube Dept, ATTN: Mr. Daniel D. Mickey, 316 East Ninth St, Owensboro, Ky

DISTRIBUTION (cont'd)

No. cys	
1	General Electric Co, Defense Systems Dept, ATTN: Mr. A. Sinisgalli, Atlantic Bldg, Syracuse, NY
1	General Electric Co, MSD, ATTN: Mr. J. Spencer, 3198 Chestnut St, Philadelphia, Pa
1	Georgia Institute of Technology and Engineering Experiment Station, ATTN: Dr. R. B. Belser, 722 Cherry Street NW, Atlanta 13, Ga
1	General Precision, Inc., Kearfott Division, ATTN: Dr. William H. Duerig, Clifton, NJ
1	General Precision Inc., Systems Division, ATTN: Dr. S. D. Black, Little Falls, NJ
1	Honeywell Inc., Aeronautical Division, 2600 Ridgway Road, Minneapolis, Minn 55440
10	Hughes Aircraft Co, Ground Systems Group, ATTN: Dr. J. E. Bell, P. O. Box 1097, Fullerton, Calif
1	Hughes Aircraft Co, ATTN: Dr. C. Perkins, Florance and Teale Streets, Culver City, Calif
5	IBM, Federal Systems Division, ATTN: W. A. Bohan, Oswego, NY
1	IIT Research Institute, Document Library, 10 West 35th St, Chicago 16, Ill
1	Institute for Defense Analysis, 1710 H Street, NW, Wash, DC
1	Institute for Defense Analysis, Research & Engineering Support Division, 1825 Connecticut Ave NW, Wash, DC
1	LTV, Vought Aeronautics Division, ATTN: H. E. Reynolds, P.O. Box 5907, Dallas, Tex
1	Lockheed Aircraft Corporation, Missile & Space Division, ATTN: Mr. Fred Barline, Dept 5872, 1111 Lockheed Way, Sunnyvale, Calif
1	Lockheed Missile & Space Co, ATTN: Mr. Harvey Duncan, Dept 62-72, 1123 North Mathilda Ave, Sunnyvale, Calif
1	Martin Company, Nuclear Division, ATTN: S. E. Harrison, Mail No. 716, Baltimore 3, Md
1	Martin Company, Nuclear Division, ATTN: Nuclear Library, Baltimore 3, Md
1	Martin Company, DATAC, Research Library A-52, Denver 1, Colo
1	Melpar Inc., 3000 Arlington Blvd, Falls Church, Va

DISTRIBUTION (cont'd)

No. cys	
	Massachusetts Institute of Technology, Lincoln Laboratory, P.O. Box 73, Lexington, Mass
1	(Document Library)
1	(E. E. Pike)
1	(O. V. Fortier)
1	New York University, ATTN: Dr. K. Kallman, Physics Dept, Washington Square, New York 3, NY
1	North American Aviation Corporation, Atomics International Division, ATTN: Dr. A. J. Saur, 21600 Van Owen Street, Canoga Park, Calif
1	North American Aviation Inc., Space & Information Systems Division, ATTN: S. Falbaum, 5555 Ferguson Street, Commerce, Calif
2	Northrop-Ventura Division, Northrop Corporation, ATTN: Dr. T. M. Hallman, 1515 Rancho Conejo Blvd, Newbury Park, Calif
1	Physics International, ATTN: Dr. F. C. Ford, 2229 Fourth St, Berkeley 10, Calif
2	Battelle Memorial Institute, Radiation Effects Information Center, ATTN: E. N. Wyler, 505 King Ave, Columbus 1, Ohio
1	Remington Rand Univac, Division of Sperry Rand Corporation, ATTN: Dr. W. D. Miller, Univac Park, St Paul 16, Minn
2	Scientific and Technical Information Facility, ATTN: NASA Representative (SAK/DL-988), P. O. Box 5700, Bethesda, Md 20014
2	Space Technology Laboratories, ATTN: Dr. B. Sussholz and Mr. J. Maxey,. 5730 Arbor Vitae Street, Los Angeles, Calif
1	Space General Corporation, ATTN: I. Doshay, El Monte, Calif
1	Sperry Gyroscope Co, Lakeville & Marcus Ave, Great Neck, JY
1	Sperry Microwave Electronics Co, ATTN: Dr. Gordon R. Harrison, P. O. Box 1828, Clearwater, Fla
1	Stevens Institute of Technology, ATTN: Dr. E. Hanley, 501 & 711 Hudson Street, Hoboken, NJ
1	Sylvania Electric Products, Inc., Emporium, Pa
1	Times Wire & Cable Division, International Silver Co, Transmission Systems Section, ATTN: Allen M. Kushner, Wallingford, Conn
1	University of British Columbia, Dept of Physics, ATTN: P. J. Sykes, Jr., Vancouver 8, British Columbia

DISTRIBUTION (cont'd)

No. cys	
1	University of Michigan, Institute of Science and Technology, ATTN: BAMIRAC, Mr. Richard Jamron, Box 618, Ann Arbor, Mich
75	University of New Mexico, Engineering Experiment Station, ATTN: Dr. W. W. Grannemann, Albuquerque, NM
1	Official Record Copy (Captain Karl H. Schumaker, WLDN)